

Solitons in graphene

Jigger Cheh^{1*} and Hong Zhao^{1,2†}

¹*Department of Physics, Institute of Theoretical Physics and Astrophysics, Xiamen University, Xiamen 361005, China and*

²*State Key Laboratory for Nonlinear Mechanics, Institute of Mechanics, Chinese Academy of Sciences, Beijing 100080, China*

In this paper we demonstrate the direct evidence of solitons in graphene by means of molecular dynamics simulations and mathematical analysis. It shows various solitons emerge in the graphene flakes with two different chiralities by cooling procedures. They are in-plane longitudinal and transverse solitons. Their propagations and collisions are studied in details. A soliton solution is derived by making several valid simplifications. We hope it shed light on understanding the unusual thermal properties of graphene.

PACS numbers: 05.45.Yv, 65.80.Ck

Solitons are localized particle-like wavepackets which preserve their identities such as shape and amplitude during propagation and after collision between them due to the compensation of nonlinearity for dispersion. Nowadays, solitons are under intense investigation in many systems including Bose-Einstein condensates, nonlinear optics, plasmas and anharmonic lattices[1–5], etc.

The role solitons played in thermal properties in low dimensional lattices such as thermal rectification and divergence of thermal conductivity has been speculated for a long time. Thermal conductivity would be direction dependent if solitons are involved. It was first theoretically introduced in 1992[6] and experimentally observed in asymmetrically mass-loaded carbon nanotubes[7] where the rectification coefficient is estimated by considering KdV solitons. Similar thermal rectification has been numerically studied in asymmetric shaped graphene[8] recently. Anomalous thermal conduction that thermal conductivity depends on the size of the system has been investigated for years[4, 5, 9–11]. Different theoretical approaches are applied to understand its mechanism[12–14]. Since solitons appear in those systems with anomalous transport properties, it is extremely important to assess whether such properties are related to solitons. Solitons are invoked to explain thermal divergence dates back to Toda in 1972[10, 15]. Later it shows solitons might be responsible energy carriers for thermal divergence[16] and the divergent exponent is dependent upon the scattering rates of solitons and soliton-phonon coupled energy diffusion process[4, 5]. Since anomalous thermal conduction was observed in both carbon nanotubes and graphene flakes[17, 18], thus it is very important to investigate whether solitons exist in graphene.

Though the thermal properties indicate solitons might exist in graphene however there is no direct evidence so far despite some theoretical work suggests the possibility of supersonic KdV solitons in carbon nanotubes and graphite[19, 20]. Recently some paper surmises the existence of possible solitons in graphene under specific conditions or configurations. Five types of solitary waves are numerically found possible along the hydrogen-terminated edge of graphene which corresponds to the molecule group CH[21]. When strain is applied spa-

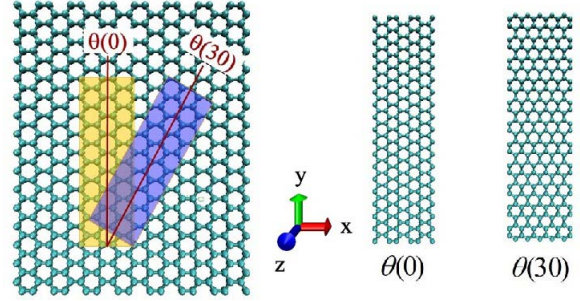


Figure 1: (Color online) Chiralities of the rectangle graphene flakes. Graphene $\theta(0)$ denotes the graphene flake with armchair edge along the x-axis and zigzag edge along the y-axis (orange flake). Since rotate Graphene $\theta(0)$ clockwise by 30° we get a new rectangle graphene flake with armchair edge and zigzag edge swapped (blue flake) thus we denote it as Graphene $\theta(30)$.

tially localized electric state might appear near the edge of graphene[22]. It is connected to a soliton solution in chiral gauge theory which describes the special state of electrons. It does not describe the lattice vibration modes. Thus in general case whether solitons would exist in graphene is still unanswered.

In this paper we demonstrate the emergence of solitons in graphene in both molecular dynamics simulations and mathematical analysis. It shows various solitons emerge in graphene flakes with two different chiralities by cooling procedures. They are in-plane longitudinal and transverse solitons. They preserve their identities such as shape and amplitude during propagations and after collisions. Their velocities are smaller than the relative sound speeds. Phase shifts are brought by an averaged acceleration effect in collision between two longitudinal or two transverse solitons. A longitudinal and a transverse soliton would simply pass through each other without any interactions. We derive a NLS (Nonlinear Schrödinger) equation to obtain the analytical soliton solution with several simplifications. The validity of the analytical results is discussed by comparing with the simulation results.

We carry out the simulations in two rectangle graphene flakes with different chiralities. As shown in Fig. 1, Graphene flake with armchair edge along the x-axis and zigzag edge along the y-axis is denoted as $\theta(0)$ and Graphene flake with zigzag edge along the x-axis and armchair edge along the

*Electronic address: jk_jigger@xmu.edu.cn

†Electronic address: zhaoh@xmu.edu.cn

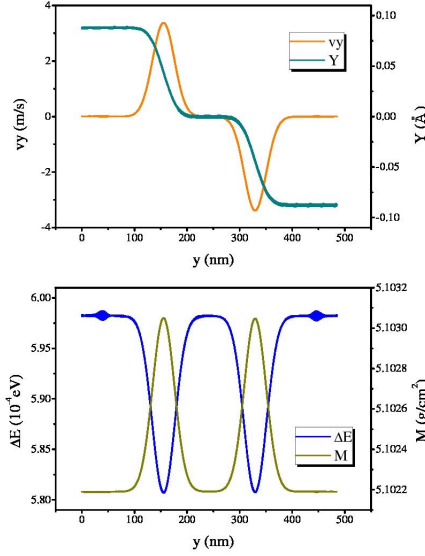


Figure 2: (Color online) Typical solitons in Graphene $\theta(0)$ are investigated. Above it shows two longitudinal solitons and their velocity and displacement distributions. Down it shows their energy and density distributions. A pair of small breather-like solitons can also be identified.

y-axis is denoted as $\theta(30)$. Graphene $\theta(0)$ contains 95952 atoms and Graphene $\theta(30)$ contains 97020 atoms. They are 485 nm long along the y-axis and 4.7 nm wide along the x-axis. Periodic boundary condition is used in the y-axis which allows solitons to propagate arbitrary long distance without boundary scattering. Periodic or free boundary condition is used in the x-axis. Free boundary condition is used in the z-axis when concerned.

We use the second-generation reactive empirical bond-order (REBO) potential[23] as implemented in the LAMMPS[24] code to simulate the anharmonic coupling between carbon atoms. We take 0.25 fs as the minimum timestep. The second-generation reactive empirical bond-order (REBO) potential[23] originates from the Brenner's potential[25] by including modified fitting data and empirical parameters. The general form of both potentials can be written as:

$$E_{ij} = V_{ij}^R(r_{ij}) + b_{ij}V_{ij}^A(r_{ij}) \quad (1)$$

Here V_{ij}^R and V_{ij}^A are repulsive and attractive pairwise potential of carbon atoms dependent upon their distance. b_{ij} is a many-body bond-order term dependent upon their bond angles and neighbor atoms. They are widely used to study diamond, fullerene, carbon nanotube and graphene, etc. Both potentials are capable of describing the short-ranged covalent-bonding C-C interactions of the carbon atoms in the same way with minor differences. It should be emphasized that, despite the effective treatment of hybridization and zero-point energy, both potentials include no explicit quantum effects. All conjugation states are derived entirely from the system geometry

and treat the electronic degrees of freedom in a purely empirical manner. Thus all the simulation results are obtained and discussed in the framework of classic mechanics.

We also test our simulations by using Tersoff potential[26] which is also a widely used empirical potential for the carbon atoms. Similar results would be obtained. It states the main results are general for the potentials describing the nonlinear interactions of carbon atoms.

To identify the solitons in graphene a new strategy is used in our simulations. Later we shall explain why such strategy works. We first thermalize the graphene flakes at a given temperature (e. g., 1-30 K) for 100 ps with Nose-Hoover thermal bath and relax for 20 ps to be equilibrated. Then we set the velocities of all atoms to zero every constant step (e. g., 100-500 fs) for hundreds of times. After those procedures various solitons emerge from graphene with different amplitudes dependent upon the initial temperature and cooling time. Using different initial conditions and time steps, the emerging solitons might be different.

We focus upon several different distributions of atoms to illustrate the identities of the emerging solitons. Velocity distributions of atoms are investigated which include longitudinal velocity (v_y) distributions and transverse velocity (v_x) distributions. They also stand for the momentum distributions when the mass of the carbon atoms is multiplied. Displacements around the equilibrium positions of the atoms which include longitudinal displacement (Y) and transverse displacement (X) are investigated. Energy distributions are investigated by considering the differences between the ground state energy ($\Delta E = E - E_0$). Density distributions are investigated by considering the reduced density M rather than density ρ for simplicity. The relation between them is:

$$\rho = 1.99 \times \frac{4\sqrt{3}}{9} M = 1.99 \times \frac{4\sqrt{3}}{9} \times \frac{1}{\langle r \rangle^2} \quad (2)$$

Here $\langle r \rangle$ is the average bond distance of an atom between its three neighbors.

The typical solitons in Graphene $\theta(0)$ are shown in Fig. 2-4. A pair of longitudinal solitons and a pair of breather-like solitons are shown in Fig. 2 and Fig. 3. A pair of longitudinal solitons and another pair of small longitudinal solitons are shown in Fig. 4.

The velocity and displacement distributions of the two main longitudinal solitons are shown in Fig. 2. Their energy and density distributions are also shown in Fig. 2. They lack energy and aggregate density towards the fluctuation background. A pair of small breather-like solitons is also identified as shown in Fig. 3. Using different initial conditions another pair of small longitudinal solitons can be identified. It is shown in Fig. 4 they aggregate energy and lack density towards the fluctuation background.

Typical solitons in Graphene $\theta(30)$ are shown in Fig. 5 and Fig. 6. A pair of transverse solitons and a pair of longitudinal solitons are identified.

The velocity and displacement distributions of the transverse and longitudinal solitons are shown in Fig. 5. The displacement distributions of the longitudinal solitons are not easy to distinguish from the background fluctuation. However

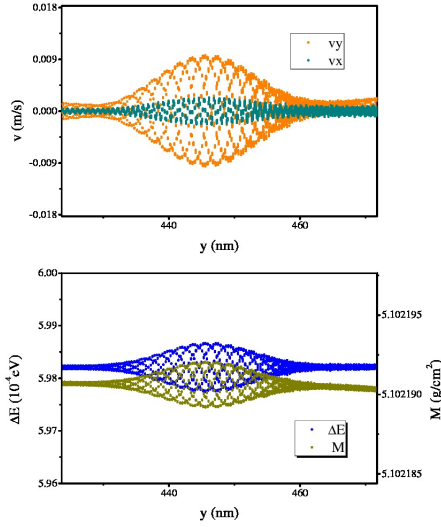


Figure 3: (Color online) The breather-like soliton is investigated. Above it shows the longitudinal and transverse velocity distributions of the breather-like soliton. Down it shows the energy and reduced density distributions of the breather-like soliton.

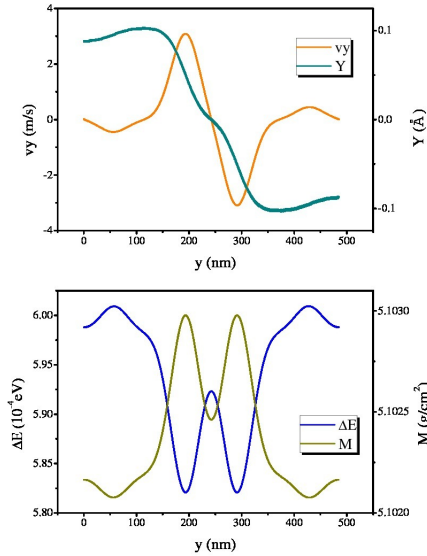


Figure 4: (Color online) Using different initial conditions, another two small solitons are identified in Graphene $\theta(0)$ They are also longitudinal solitons.

their shapes resemble the longitudinal solitons in Graphene $\theta(0)$ as well. Their energy and density distributions are shown in Fig. 6. The transverse solitons aggregate energy and lack density. The longitudinal solitons lack energy towards the background. When two transverse solitons collide together we can identify them lacking of density then.

Due to the momentum conservation solitons emerge in pairs with opposite velocity localization value. Since the graphene

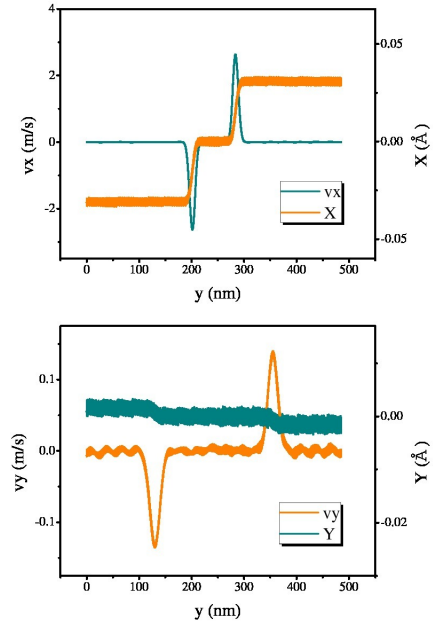


Figure 5: (Color online) Typical solitons in Graphene $\theta(30)$ are investigated. Above it shows the velocity and displacement distributions of the transverse solitons. Down it shows the velocity and displacement distributions of the longitudinal solitons.

flakes have no compression or stretching the total displacements are also zero. The lengths of some solitons are comparable with the mean free path of phonons[27]. It indicates a long length might be needed to consider the contribution of solitons in thermal conduction. We only observe random fluctuations in out-of-plane distribution. Such difference might affect thermal conduction when flexural modes are enhanced or suppressed[28].

In order to confirm the wave profiles are solitons we have to study their propagation and collision. Solitons shall preserve their identities in propagation and after collision. It is the usual way to identify soliton nature in nonlinear kinetics. It is shown in Fig. 7-10 how solitons propagate and collide in the graphene flakes. The propagation and collision of the longitudinal and breather-like solitons in Graphene $\theta(0)$ are shown in Fig. 7 and Fig. 8. The propagation and collision of the transverse and longitudinal solitons in Graphene $\theta(30)$ are shown in Fig. 9 and Fig. 10.

It is shown in Fig. 7 the propagation and collision of the longitudinal solitons with different amplitudes in Graphene $\theta(0)$. Their propagating velocity is 20.0 km/s and it is smaller than the longitudinal sound speed which is 21.3 km/s[29]. The propagation velocity is close to the sound speed. The propagating velocity seems insensitive to the amplitudes. Their collisions are elastic without changing their identities. It confirms they are solitons.

It is shown in Fig. 8 the propagation of the breather-like solitons in Graphene $\theta(0)$. Their propagating velocity is 5.0 km/s. Their collisions are also elastic.

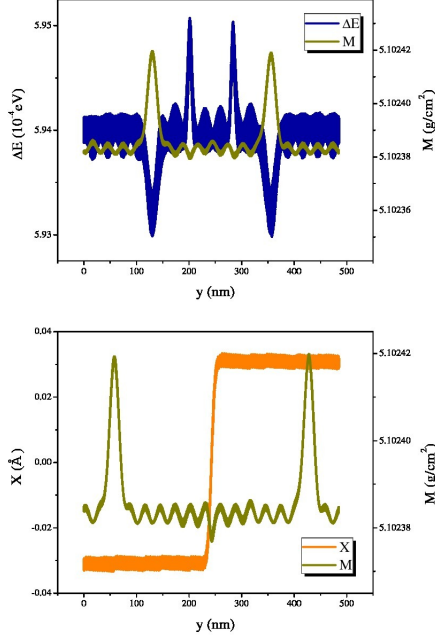


Figure 6: (Color online) Typical solitons in Graphene $\theta(30)$ are investigated. Above it shows the energy and density distributions of the transverse and longitudinal solitons. Down it shows the energy and density distributions when the two longitudinal soliton collide together.

It is shown in Fig. 9 the propagation and collision of the transverse solitons in Graphene $\theta(30)$. It is shown in Fig. 10 the propagation and collision of the longitudinal solitons in Graphene $\theta(30)$. The propagating velocity of transverse solitons is 11.4 km/s. The propagating velocity of the longitudinal solitons is 20.0 km/s. Both velocities are smaller than the relative sound speed which is 21.3 km/s (longitudinal sound speed) and 13.6 km/s (transverse sound speed)[29]. Their propagating velocities are also weakly dependent upon the amplitudes. Their collisions are elastic as well.

Solitons shall have interactions (decelerations and accelerations) in collisions due to nonlinearity. It is distinctively different from linear waves which have no interactions due to superposition principle. Solitons would deviate from their original trajectories due to collisions. They are not in the position which would be anticipated by extending their original trajectories. It means solitons are phase-shifted. Phase shift is a well known behavior of solitons in collisions[30, 31].

It is shown in Fig. 11 the spatial-temporal trajectories of the longitudinal solitons in Graphene $\theta(0)$. Straight lines are observed before or after collision. In collision, solitons are first decelerated and then accelerated by a spatial jump. The average propagating velocity is 22.3 km/s during collision thus solitons exhibit an averaged acceleration effect. The dash lines represent the original trajectories of the solitons assuming there was no collision. It clearly illustrates the averaged acceleration effect brings forth the phase shift of soli-

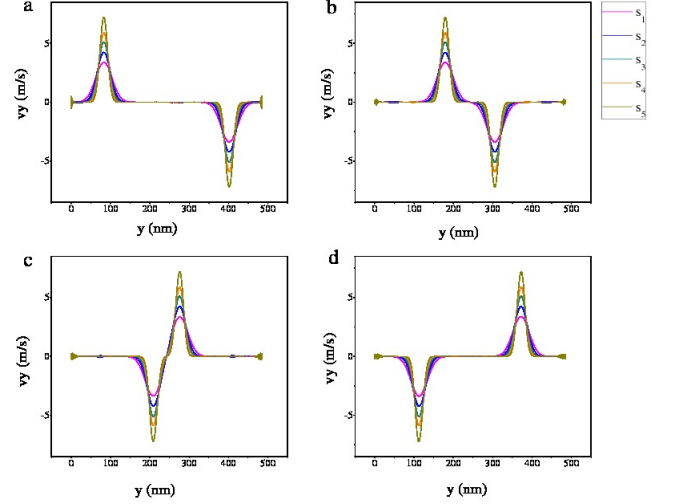


Figure 7: (Color online) Propagation and collision of the two longitudinal solitons in Graphene $\theta(0)$ with different amplitudes. The time interval between two neighboring events is 4.8 ps from (a) to (d).

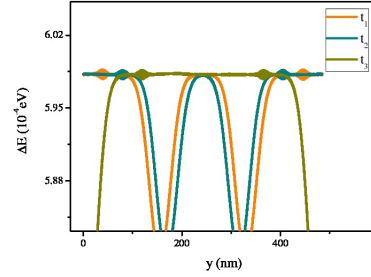


Figure 8: (Color online) Propagation of the breather-like solitons in Graphene $\theta(0)$. The time interval is 8 ps between two neighboring events.

tons. Spatial jumps are also the important behavior of solitons in collision[31]. It is shown in Fig. 11 how the spatial jump happens. Since we identify the position of solitons according to the extreme value points. So it is difficult to do so in some critical moments when there are four extreme value points. It behaves like a spatial jump if we neglect those moments.

It is shown in Fig. 12 the spatial-temporal trajectories of two transverse and two longitudinal solitons in Graphene $\theta(30)$. The transverse solitons are first decelerated and then accelerated by a spatial jump in collision. The averaged propagating velocity is 13.9 km/s during collision. It exhibits an averaged acceleration effect in collision. The phase shift of the transverse solitons is clearly illustrated by the dash lines. Similar behaviors are also observed in collision between two longitudinal solitons. The averaged propagating velocity is 22.3 km/s in collision during collision. The phase shift of the longitudinal solitons is also clearly illustrated by the dash lines.

It is shown in Fig. 13 the spatial-temporal trajectories of

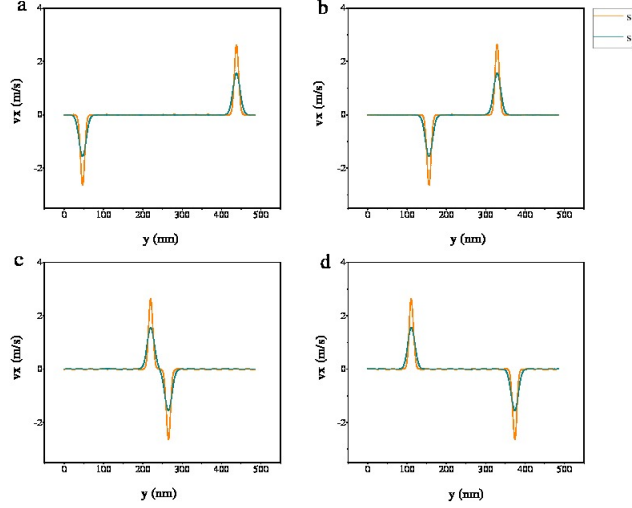


Figure 9: (Color online) Propagation and collision of the transverse solitons in Graphene $\theta(30)$ with different amplitudes. The time interval between two neighboring events is 9.6 ps from (a) to (d).

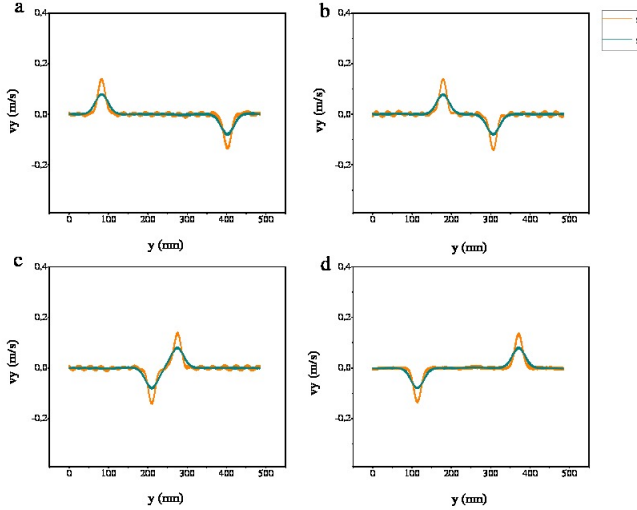


Figure 10: (Color online) Propagation and collision of the longitudinal solitons in Graphene $\theta(30)$ with different amplitudes. The time interval between two neighboring events is 4.8 ps from (a) to (d).

a transverse soliton and a longitudinal soliton in Graphene $\theta(30)$. It describes the collision between a transverse soliton and a longitudinal soliton. Unlike collision between two transverse solitons or two longitudinal solitons, they would simply pass through each other without any interactions. Thus only straight lines are observed in their trajectories.

Using different initial conditions and cooling time steps even more solitons might emerge in graphene with similar kinetic properties. It is shown in Fig. 14 and Fig. 15.

The emergence of solitons is observed by cooling procedures. It is quite different from the usual way in which solitons are generated by imposing a strong impulse upon the

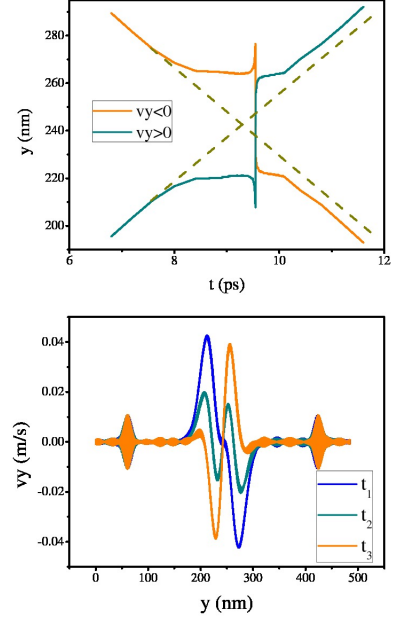


Figure 11: (Color online) Above it shows the spatial-temporal trajectories of two longitudinal solitons in Graphene $\theta(0)$. Dash lines are added as auxiliary lines to illustrate the original trajectories of the solitons assuming there was no collision. Down it shows the velocity distributions around the spatial jump. The time interval between the two neighboring events is 0.0075 ps. t_2 is the critical moment in the spatial jump.

lattice[31, 32]. Thus a different theoretical approach is required to obtain the soliton solution. Here we use the multiscale asymptotic method to derive a NLS equation to describe the nonlinear process in graphene. Multiscale asymptotic method first developed in 1969[33] assumes all higher-order harmonics are small enough so that the fundamental frequencies determine the kinetic behaviors of the system. It is widely used in different nonlinear systems to obtain soliton solutions[34–36].

We use the Brenner's potential[25] to describe the interactions between carbon atoms in the analytical model here. It is the 1st simplification in our analytical model.

Here we take Graphene $\theta(0)$ as an example to obtain the soliton solution. Following similar steps[19, 20] we expand the interatomic potential into Taylor series up to fourth order around the equilibrium position in Graphene $\theta(0)$. For simplicity only the longitudinal displacement Y is considered. It is the 2nd simplification in our analytical model.

The Hamiltonian is $H = H_0 + \sum_{n=1}^{N_l} H_n$ where H_n is the perturbation energy in n th layer. Thus $H_n = m_n H_n^a$ where m_n is the number of atoms in n th layer and we get

$$H_n^a = \frac{b}{2}(Y_{n+1} - Y_n)^2 - \frac{bp}{3}(Y_{n+1} - Y_n)^3 + \frac{bq}{4}(Y_{n+1} - Y_n)^4 \quad (3)$$

Here $Y_n = y_n - Y_{n0}$ is the longitudinal displacements of atoms around their equilibrium position in n th layer and $b = 58.93 \text{ eV}$, $p = 2.796$, $q = 1.990$.

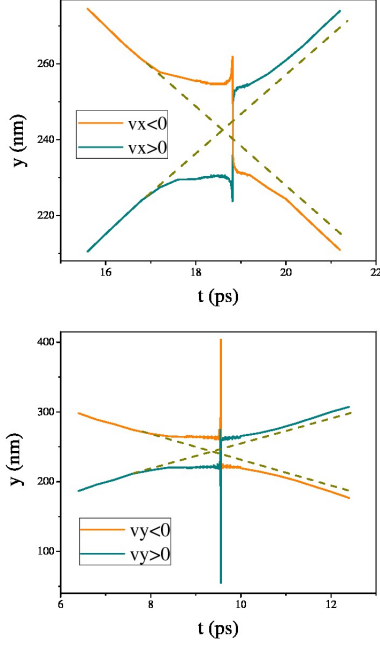


Figure 12: (Color online) Above it shows the spatial-temporal trajectories of two transverse solitons in Graphene $\theta(30)$. Down it shows the spatial-temporal trajectories of two longitudinal solitons in Graphene $\theta(30)$. Dash lines are added as auxiliary lines to illustrate the original trajectories of the solitons assuming there was no collision.

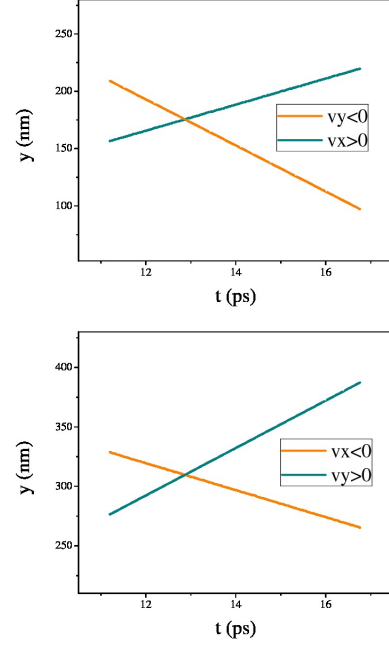


Figure 13: (Color online) Above it shows the spatial-temporal trajectories of a transverse soliton propagate forward and collide with a longitudinal soliton in Graphene $\theta(30)$. Down it shows the spatial-temporal trajectories of a transverse soliton propagate backward and collide with a longitudinal soliton in Graphene $\theta(30)$.

Then we can get the kinetic equation to describe the longitudinal motion as:

$$m \frac{d^2 Y_n}{dt^2} = \frac{b}{l_0^2} [Y_{n+1} - 2Y_n + Y_{n-1}] - \frac{bp}{l_0^2} [(Y_{n+1} - Y_n)^2 - (Y_n - Y_{n-1})^2] + \frac{bq}{l_0^2} [(Y_{n+1} - Y_n)^3 - (Y_n - Y_{n-1})^3] \quad (4)$$

Here $m = 1.99 \times 10^{-26} \text{ kg}$ and $l_0 = 1.212 \text{ \AA}$ which is the equilibrium distance between two layers.

We then expand the displacement by small excitations up to first-order perturbation term

$$Y_n = \sum_{v=1}^{\infty} \epsilon^v u_n^{(v)}(\tau, \xi_n, \phi_n) \approx \epsilon u_n^{(1)}(\tau, \xi_n, \phi_n) \quad (5)$$

Here $u_n^{(1)} = \sum_{l=-\infty}^{\infty} u_{n,l}^{(1)}(\tau, \xi_n) \exp(il\phi_n)$ is expanded in harmonic terms with $\tau = \sqrt{\frac{b}{ml_0^2}} \epsilon^2 t$, $\xi_n = \epsilon n l_0 - \lambda \tau / \epsilon$, $\phi_n = kn l_0 - \omega \tau / \epsilon^2$.

Here we simplify the expansions again by neglecting the high-order harmonics $u_{n,l}^{(1)}(\tau, \xi_n) = 0$, if $|l| > 1$. It is the 3rd simplification in our analytical model.

Substituting $Y_n = \epsilon u_{n,0}^{(1)}(\tau, \xi_n) + \epsilon u_{n,1}^{(1)}(\tau, \xi_n) \exp(i\phi_n) + \epsilon u_{n,1}^{(1)*}(\tau, \xi_n) \exp(-i\phi_n)$ into the kinetic equation and equating the coefficients of ϵ . After that we derive the following equation:

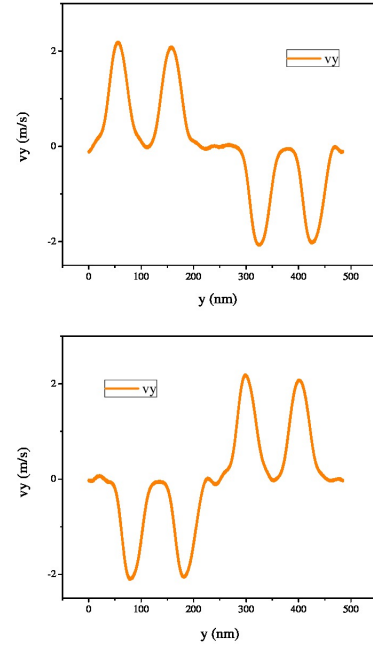


Figure 14: (Color online) Four solitons in Graphene $\theta(0)$. The interval between the two neighboring events is 12 ps.

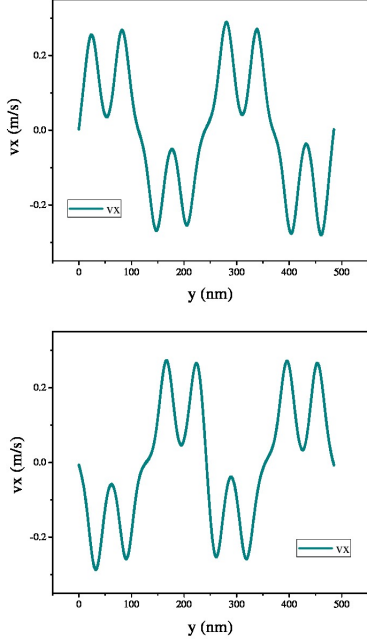


Figure 15: (Color online) Eight solitons in Graphene $\theta(30)$. The interval between the two neighboring events is 10 ps.

$$i \frac{\partial u_{n,1}^{(1)}}{\partial \tau} = \frac{\omega_0^2}{8} \frac{\partial^2 u_{n,1}^{(1)}}{\partial \xi_n^2} + [\frac{3}{2} q \omega^3 - \omega p^2 (4 + \omega^2)] |u_{n,1}^{(1)}|^2 u_{n,1}^{(0)} + 8 \omega C p^2 u_{n,1}^{(1)} \quad (6)$$

Here C is an integration constant. By substituting variables it is reduced to a standard cubic NLS equation:

$$i \frac{\partial \psi}{\partial \eta} - \frac{\sigma}{2} \frac{\partial^2 \psi}{\partial \delta^2} + |\psi|^2 \psi = 0 \quad (7)$$

Here $\psi = \exp(i8p^2 \omega \int C d\tau) u_{n,1}^{(1)}$, $\sigma = \frac{1}{(p^2 - \frac{3}{2}q)\omega^2 + 4p^2}$, $\eta = \omega \tau / \sigma$, $\delta = \frac{2}{l_0} \xi_n$. Here we have $\sigma = \frac{1}{4.83\omega^2 + 31.3} > 0$ which means it is a normal NLS equation.

A soliton solution is possible in the NLS equation above:

$$Y_n = A [\cos X - 2p\sqrt{\sigma} \tanh \Theta - A \tan \phi \sin X + A'] \quad (8)$$

Here A' is an integration constant and A , α , ϕ are free parameters. v_1 is the propagation velocity of the soliton.

$$X = knl_0 + 2\alpha - [2\alpha \cos \frac{kl_0}{2} + (2 - \alpha^2 - \frac{A^2}{2\sigma \cos^2 \phi} + \frac{4p^2 A^2}{\cos^2 \phi}) \sin \frac{kl_0}{2}] \sqrt{\frac{b}{ml_0^2}} t$$

$$\Theta = \frac{A}{\sqrt{\sigma}} (nl_0 - tv_1)$$

$$v_1 = [\cos \frac{kl_0}{2} - (\alpha + \frac{A \tan \phi}{2\sqrt{\sigma}}) \sin \frac{kl_0}{2}] \sqrt{\frac{b}{m}}$$

$$y_n = Y_n + Y_{n0} = Y_n + nl_0$$

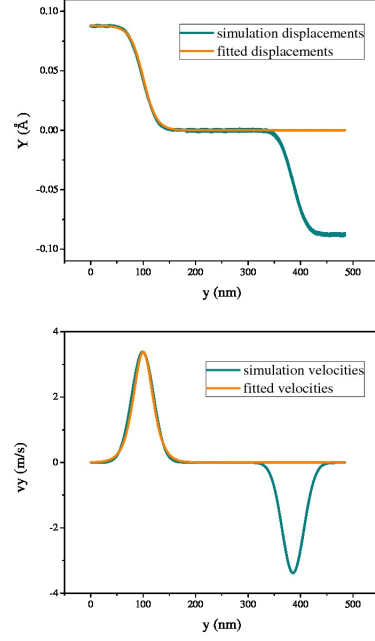


Figure 16: (Color online) Comparing the analytical soliton solution with the soliton obtained in simulations. Above it shows the displacement distribution agrees with the simulation results. Down it shows the velocity distribution also agrees with the simulation results.

The complete form of the soliton solution is complicated. It can be further simplified by considering the kinetic properties of solitons in the molecular simulations. From the previous study, we know the velocities of the solitons are insensitive to the amplitudes. Thus the amplitude dependent parameter in v_1 might be neglected. It means $\tan \phi = 0$ here. It is the 4th simplification in our analytical model.

The propagating velocities of solitons are close to the relative sound speed. It also can be used as a valid simplification. The relative sound speed is $v_2 = \sqrt{\frac{b}{m}}$. It means $v_1 \cong v_2$. It is the 5th simplification in our analytical model.

From the 5th simplification we can obtain

$$[\cos \frac{kl_0}{2} - (\alpha + \frac{A \tan \phi}{2\sqrt{\sigma}}) \sin \frac{kl_0}{2}] \sqrt{\frac{b}{m}} \cong \sqrt{\frac{b}{m}} \quad (9)$$

Taking the 4th simplification into account, we have

$$\cos \frac{kl_0}{2} - \alpha \sin \frac{kl_0}{2} \cong 1 \quad (10)$$

So we may obtain the following relation that:

$$\cos \frac{kl_0}{2} \cong 1, \sin \frac{kl_0}{2} \cong 0, \alpha \ll 1 \quad (11)$$

Taking $\tan \phi = 0$, $\cos \frac{kl_0}{2} \cong 1$, $\sin \frac{kl_0}{2} \cong 0$ and $\alpha \ll 1$ into Eq. 8, we finally can obtain the soliton solution in the continuum approach as:

$$Y = A_0 \tanh[c(y - tv_1)] + A' \quad (12)$$

Here A_0 and c are determined by the anharmonic parameters p and q in Eq. 3.

$$A_0 = A(\sqrt{1-4\alpha^2} - 2p\sqrt{\sigma}) = A(\sqrt{1-4\alpha^2} - \sqrt{\frac{4p^2}{(p^2-\frac{3}{2}q)\omega^2+4p^2}}) \quad (13)$$

$$c = A/\sqrt{\sigma} = A\sqrt{(p^2-\frac{3}{2}q)\omega^2+4p^2} \quad (14)$$

The relative longitudinal velocity distribution of the soliton solution is:

$$vy = \frac{dy}{dt} = -A_0cv_1\text{sech}^2[c(y-tv_1)] \quad (15)$$

In a given time t_0 the relative soliton solution should be:

$$Y = A_0\tanh[c(y-y_0)] + A' \quad (16)$$

$$vy = -A_0cv_1\text{sech}^2[c(y-y_0)] \quad (17)$$

To investigate the validity of our analytical results, we first try to fit the soliton obtained in the simulation with the soliton solution we derived. Next we try to use the fitted soliton solutions as the initial conditions to investigate the propagation and collision of the fitted solitons.

We first fit the displacement distribution to determine A_0 , c and A' . When the parameters are obtained we use them to fit the velocity distribution. The fitted displacement and velocity distributions ($v_1 = 20.0$ km/s) are:

$$Y = -0.044\tanh[0.04(y-100)] + 0.044 \quad (18)$$

$$vy = 3.5\text{sech}^2[0.04(y-100)] \quad (19)$$

It is shown in Fig. 16 the results fit the left side soliton well. The right side soliton can also be well fitted in the same way. Next we use the fitted solitons as the initial conditions to investigate their propagation and collision properties. It is shown in Fig. 17 that the propagation and collision properties of the fitted solitons are almost the same as the solitons obtained in the previous molecular dynamics simulations. It states the derived soliton solution can describe the solitons obtained in the molecular dynamics simulations well.

It is well known there are extreme difficulties to obtain a soliton solution without making proper simplifications. Using different methods and simplifications, different soliton solutions might be obtained. To derive the soliton solution we use five simplifications. Thus it is important to understand the conditions our simplifications correspond to and the limits of these simplifications.

The 1st simplification is to use the Brenner's potential instead of the second-generation reactive empirical bond-order (REBO) potential. As we point out both potentials describe the short-ranged covalent-bonding C-C interactions of the carbon atoms in the same way. Our simulation results are general for the potentials describing the C-C interactions. Thus this simplification brings no significant differences.

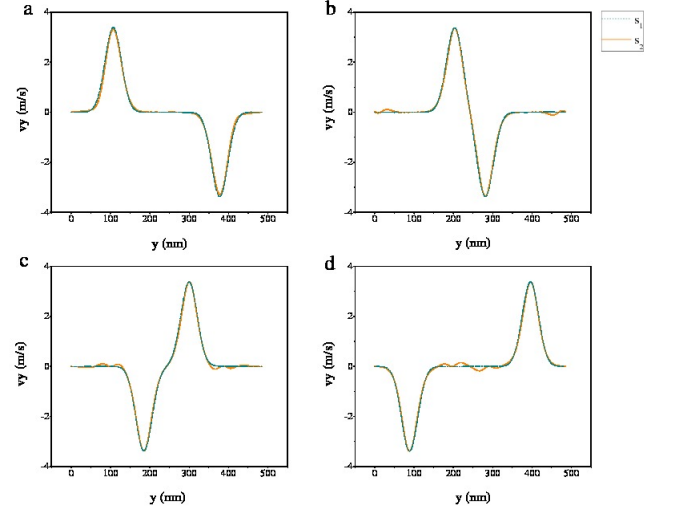


Figure 17: (Color online) s_1 is the solitons obtained in the previous molecular dynamics simulations by cooling procedures. s_2 is the solitons derived in the analytical results. The propagation and collision properties resemble each other well.

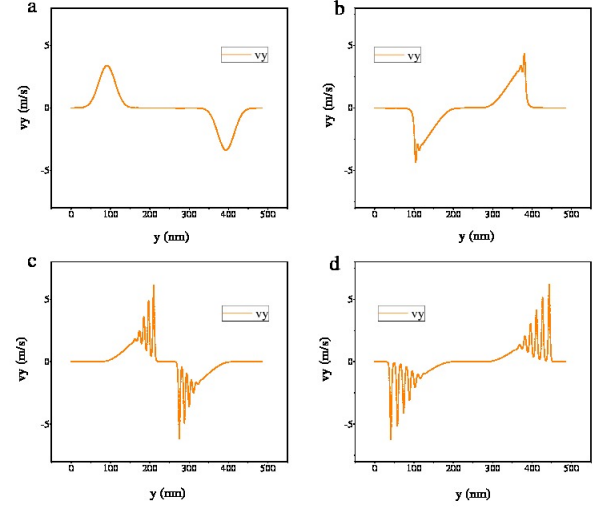


Figure 18: (Color online) Long time behavior of the longitudinal solitons in Graphene $\theta(0)$. The time interval between two neighboring events is 1.2 ns from (a) to (d).

The 2nd simplification is to consider the displacements only in one direction. It is due to the fact that only transverse/longitudinal solitons would interact with each other while a transverse soliton would not interact with a longitudinal soliton. It simplifies the graphene flakes as a quasi-one dimensional chain. However in the molecular dynamics simulations, displacements of all directions are considered. Thus our analytical model is insufficient to describe the breather-like solitons (Fig. 3) obtained in the simulations. In order to uncover the origin of the breather-like soliton, a coupled NLS equation considering both transverse and longitudinal

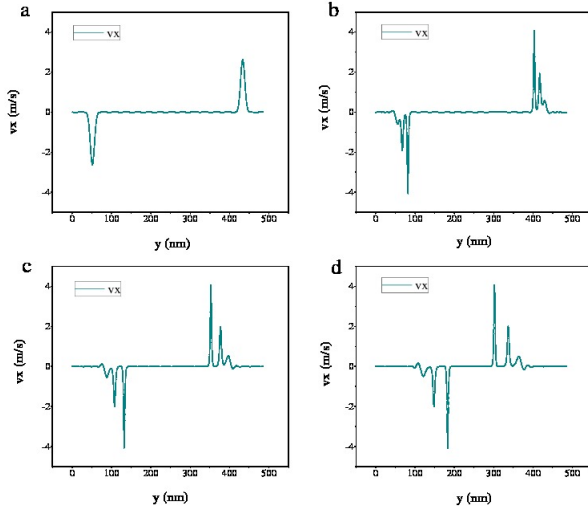


Figure 19: (Color online) Long time behavior of the transverse solitons in Graphene $\theta(30)$. The time interval between two neighboring events is 1.2 ns from (a) to (d).

displacements might be needed.

The 3rd simplification is to neglect the high-order harmonics in graphene. It is due to the fact that the high-frequency modes are suppressed in the molecular dynamics simulations by the cooling procedures. Here it also explains why such strategy works. However high-order harmonics may take part in the solitons obtained in the simulations as well. Thus the single soliton solution might be just an approximation for a multiple soliton solution. If it is so after a long time the solitons may split into several secondary solitons if their velocities are amplitude dependent. It brings us to the 4th simplification.

The 4th simplification is to neglect the velocity amplitude dependent parameter. It is a valid simplification according to Fig. 7, Fig. 9 and Fig. 10. But should the velocities of the solitons be absolutely amplitude independent or weakly amplitude dependent still remain unanswered. To answer that question we need to investigate the long time behaviors of the solitons. Thus we keep the solitons propagate as long as about 4 ns. The total propagation distance of the longitudinal solitons is more than 0.1 mm. The total propagation distance of the transverse solitons is more than 0.05 mm. It is shown in Fig. 18 the longtime behavior of the longitudinal solitons in Graphene $\theta(0)$. It is shown in Fig. 19 the longtime behavior of the transverse solitons in Graphene $\theta(30)$. They gradually split into several secondary solitons arranged in a train with increasing or decreasing amplitudes. If the velocities are proportional to the amplitudes they would appear with increasing amplitudes arrayed in a straight line. Meanwhile if the velocities are inversely proportional to the amplitudes they would appear with decreasing amplitudes arrayed in a straight line. So it is shown in Fig. 20 the velocities of the longitudinal solitons are proportional and the transverse solitons are inversely proportional to the amplitudes.

The 5th simplification is to assume the soliton velocity is close to the relative sound speed. The propagating velocity

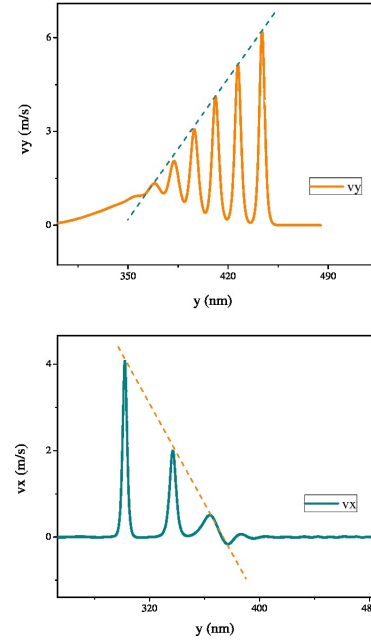


Figure 20: (Color online) Above it shows the longitudinal solitons are arranged in a train with increasing amplitudes. Their amplitudes appear in a straight line. Down it shows the transverse solitons are arranged in a train with decreasing amplitudes. Their amplitudes also appear in a straight line.

of the longitudinal solitons is 20.0 km/s and the propagating velocity of the transverse solitons is 11.4 km/s. Both velocities are close to the relative sound speed which is 21.3 km/s and 13.6 km/s.

In summary, various solitons would emerge in the graphene flakes by cooling procedures. They are subsonic transverse and longitudinal solitons. They exhibit an averaged acceleration effect in collision which means they are phase-shifted. A soliton solution is derived by taking several simplifications which correspond to the simulation conditions. The validity of the soliton solution is confirmed by comparing with simulation results. When periodic boundary condition is used in x-axis, the graphene flakes resemble simplified carbon nanotubes. Similar solitons might be also important in carbon nanotubes. We hope our work shed light on understanding the unusual thermal properties of graphene and other similar materials and also benefit the development of graphene based thermal device.

Acknowledgments

This work was supported by National Natural Science Foundation of China (#10925525 and #10775115), and National Basic Research Program of China (973 program) (#2007CB814800).

-
- [1] C. Becker et al., Nature Phys. **4**, 496-501 (2008)
 - [2] F. Lederer et al., Phys. Rep. **463**, 1-126 (2008)
 - [3] R. Heidemann, S. Zhdanov, R. Sutterlin, H. M. Thomas, and G. E. Morfill, Phys. Rev. Lett. **102**, 135002 (2009)
 - [4] H. Zhao, Z. Wen, Y. Zhang, and D. Zheng, Phys. Rev. Lett. **94**, 025507 (2005)
 - [5] H. Zhao, Phys. Rev. Lett. **96**, 140602 (2006)
 - [6] T. Iizuka, and M. Wadati, J. Phys. Soc. Jpn. **61**, 3077 (1992)
 - [7] C. W. Chang, D. Okawa, A. Majumdar, and A. Zettl, Science **314**, 1121-1124 (2006)
 - [8] J. Hu, X. Ruan, and Y. P. Chen, Nano Lett. **9**, 2730-2735 (2009); N. Yang, G. Zhang, B. Li, Appl. Phys. Lett. **95**, 033107 (2009)
 - [9] S. Lepri, R. Livi, and A. Politi, Phys. Rev. E **68**, 067102 (2003); T. Mai, A. Dhar, and O. Narayan, Phys. Lett. **98**, 184301 (2007); D. Xiong, J. Wang, Y. Zhang, and H. Zhao, Phys. Rev. E **82**, 030101(R) (2010)
 - [10] S. Lepri, R. Livi, and A. Politi, Phys. Rep. **377**, 1-80 (2003)
 - [11] A. Dhar, Advances in Physics **57**, 457-537 (2008)
 - [12] T. Prosen and D. K. Campbell, Phys. Rev. Lett. **84**, 2857 (2000)
 - [13] P. Cipriani, S. Denisov, and A. Politi, Phys. Rev. Lett. **94**, 244301 (2005);
 - [14] F. Piazza and S. Lepri, Phys. Rev. B **79**, 094306 (2009)
 - [15] M. Toda, Phys. Scr. **20**, 424 (1979)
 - [16] F. Zhang, D. J. Isbister, and D. J. Evans, Phys. Rev. E **61**, 3541 (2000); F. Zhang, D. J. Isbister, and D. J. Evans, Phys. Rev. E **64**, 021102 (2001); K. Aoki and D. Kusnezov, Phys. Rev. Lett. **86**, 4029 (2001)
 - [17] C. W. Chang, D. Okawa, H. Garcia, A. Majumdar, and A. Zettl, Phys. Rev. Lett. **101**, 075903 (2008); A. V. Savin, B. Hu, and Y. S. Kivshar, Phys. Rev. B **80**, 195423 (2009)
 - [18] D. L. Nika, S. Ghosh, E. P. Pokatilov, and A. A. Balandin, Appl. Phys. Lett. **94**, 203103 (2009); Z. Guo, D. Zhang, and X. Gong, Appl. Phys. Lett. **95**, 163103 (2009)
 - [19] T. Y. Astakhova, O. D. Gurin, M. Menon, and G. A. Vinogradov, Phys. Rev. B **64**, 035418 (2001); T. Y. Astakhova, M. Menon, and G. A. Vinogradov, Phys. Rev. B **70**, 125409 (2004)
 - [20] A. V. Savin, and O. I. Savina, Phys. Solid State **46**, 383-391 (2004)
 - [21] A. V. Savin, and Y. A. Kivshar, EPL **89**, 46001 (2010)
 - [22] K. Sasaki, R. Saito, M. S. Dresselhaus, K. Wakabayashi, and T. Enoki, New J. Phys. **12**, 103015 (2010)
 - [23] D. W. Brenner et al., J Physics: Condensed Matter. **14**, 783-802 (2002)
 - [24] S. Plimpton, J. Comput. Phys. **117**, 1-19 (1995)
 - [25] D. W. Brenner, Phys. Rev. B **42**, 9458 (1990)
 - [26] J. Tersoff, Phys. Rev. B **37**, 6991 (1988)
 - [27] S. Ghosh et al., Appl. Phys. Lett. **92**, 151911 (2009)
 - [28] J. H. Seol et al., Science **328**, 213-216 (2010); W. Cai et al., Nano Lett. **10**, 1645-1651 (2010)
 - [29] D. L. Nika, E. P. Pokatilov, A. S. Askerov, and A. A. Balandin, Phys. Rev. B **79**, 155413 (2009)
 - [30] P. G. Drazin, and R. S. Johnson, *Solitons: an Introduction* (Cambridge University Press, Cambridge, 1989)
 - [31] K. Nakajima, H. Mizusawa, Y. Sawada, H. Akoh and S. Takada, Phys. Rev. Lett. **65**, 1667 (1990); T. Jin, H. Zhao, and B. Hu, Phys. Rev. E **81**, 037601 (2010)
 - [32] Z. Wen and H. Zhao, Chin. Phys. Lett. **22**, 1341 (2005)
 - [33] T. Taniuti, and N. Yajima, J. Math. Phys. **10**, 1369 (1969); T. Taniuti, and K. Nishihara, *Nonlinear Waves* (Pitman, Boston, 1983)
 - [34] Y.S. Kivshar, and B. Luther-Davies, Phys. Rep. **298**, 81 (1998);
 - [35] S. Flach, and C. R. Willis, Phys. Rep. **295**, 181-264 (1998);
 - [36] B. Hu, G. Huang and M. G. Velarde, Phys. Rev. E **62**, 2827 (2000)